

High-resolution study of the $^{12}\text{C}(\gamma, p\gamma')^{11}\text{B}$ reaction using a HpGe detector to resolve excited states of ^{11}B through the observation of their γ -ray decays

S. A. Morrow,^{1,*} D. Branford,^{1,†} K. Föhl,¹ J. C. McGeorge,² J.-O. Adler,³ K. Hansen,³ L. Isaksson,³ M. Lundin,³ I. J. D. MacGregor,² and B. Schroder³

¹*School of Physics, University of Edinburgh, Edinburgh EH9 3JZ, United Kingdom*

²*Department of Physics and Astronomy, University of Glasgow, Glasgow G12 8QQ, United Kingdom*

³*Department of Nuclear Physics, University of Lund, S-223 62 Lund, Sweden*

(Received 23 December 2005; published 27 April 2006)

Relative populations of states in ^{11}B following the $^{12}\text{C}(\gamma, p)^{11}\text{B}$ reaction have been measured with high resolution using a 70% HpGe γ detector to observe decay γ rays from the residual nucleus. The triplet of states near 7 MeV in ^{11}B are resolved and the measured populations compared to previous data. The analysis includes a consideration of γ -proton angular correlations, which was not made in the previous measurement. The new and previous results corrected for angular correlation effects agree reasonably well with calculations that include one- and two-body nuclear currents, pion exchange, and Δ currents, under the assumption that the photons are mainly absorbed on exchanged pions.

DOI: [10.1103/PhysRevC.73.044611](https://doi.org/10.1103/PhysRevC.73.044611)

PACS number(s): 25.20.Lj, 27.20.+n

I. INTRODUCTION

Many experiments on single-proton knockout from nuclei have been performed above the giant resonance region but below the pion threshold with electromagnetic probes, using both real and virtual photons (for example, Refs. [1–9]). In quasielastic kinematics, the $(e, e'p)$ reaction excites predominantly one-hole ($1h$) states relative to the target nucleus and the cross sections are well described assuming a direct-knockout (DKO) mechanism. However, the magnitudes of the (γ, p) data are poorly described by nonrelativistic DKO calculations, the experimental results being higher by a factor $F = 2-10$ than the DKO calculations for nuclei in the range $A = 9-209$ [6–9]. In addition, the (γ, p) reaction is observed in some cases to excite more complicated states than $1h$, suggesting that the reaction mechanism is more complex than DKO.

Numerous reaction mechanisms and kinematic effects have been considered to explain the high (γ, p) reaction strength, such as (i) photon absorption on p - n pairs, as parametrized by the quasideuteron model (QDM) [10]; (ii) photon absorption on $T = 1$ p - n pairs [11,12]; (iii) coupled-channels (two-step) processes [13]; (iv) relativistic effects [14–18]; and (v) photon absorption on a nucleon pair via meson exchange currents [19, 20]. The latter calculations appear to give the most successful description of the data.

Tests of these models have been provided by studies of the $^{12}\text{C}(\gamma, p)$ reaction ($E_\gamma = 40-100$ MeV), which strongly excites a group of one-particle two-hole ($1p2h$) states in ^{11}B at ~ 7 MeV excitation energy. [11,21–26]. The triplet of states involved have excitation energies of 6.74 MeV ($J^\pi = 7/2^-$), 6.79 MeV ($1/2^+$), and 7.29 MeV ($5/2^+$) in ^{11}B [27]. Unfortunately, definite conclusions could not be

reached for many years because the experiments did not have sufficiently high energy resolutions to determine precisely which members of the 7-MeV triplet are excited and in what proportions. This problem was overcome in 1998 through a pioneering experiment by Kuzin *et al.* [20], who used decay γ rays to identify which states in ^{11}B were excited. For their measurement, protons were detected using plastic scintillator ΔE detectors with CsI E detectors, and coincident ^{11}B decay γ rays were detected using NaI detectors. The result showed that the $7/2^-$ state carries most strength in the triplet in agreement with the two-step calculations of Ref. [13] and the predictions of the model [19,20], which assumes that photons are mainly absorbed on exchange currents.

Although the validity of these results are not in doubt, we noted that the resolution of the NaI detectors was barely adequate to resolve the decay γ rays of interest and the relative populations of the ^{11}B states were by necessity based on a consideration of the weaker γ cascades through intermediate states. In view of the fact that a knowledge of the relative populations of these ^{11}B states appears to be important to understanding the (γ, p) reaction mechanism, we considered a further study of the $^{12}\text{C}(\gamma, p\gamma')^{11}\text{B}$ reaction was worthwhile. For our new measurement we used double-sided Si strip ΔE detectors (DSSDS) in conjunction with a HpGe E detector to detect protons and a 70% HpGe to detect ^{11}B decay γ rays. The geometry was chosen to minimize the Doppler broadening effects such that the strongest γ decays from the triplet of states at ~ 7 MeV to the ^{11}B ground state could be resolved as well as the γ rays from cascades through intermediate states. A second aim of the experiment was to establish if decay γ rays following a photonuclear reaction can be observed using a HpGe γ detector in a close geometry, which has the potential to allow very closely spaced levels in the residual system to be resolved. The experiment and results are described in the next two sections. This is followed by a comparison with the measurement of Kuzin *et al.* [20] and a discussion of all the results.

*Electronic address: s.a.morrow@gmail.com

†Electronic address: db@ph.ed.ac.uk

PLAN VIEW

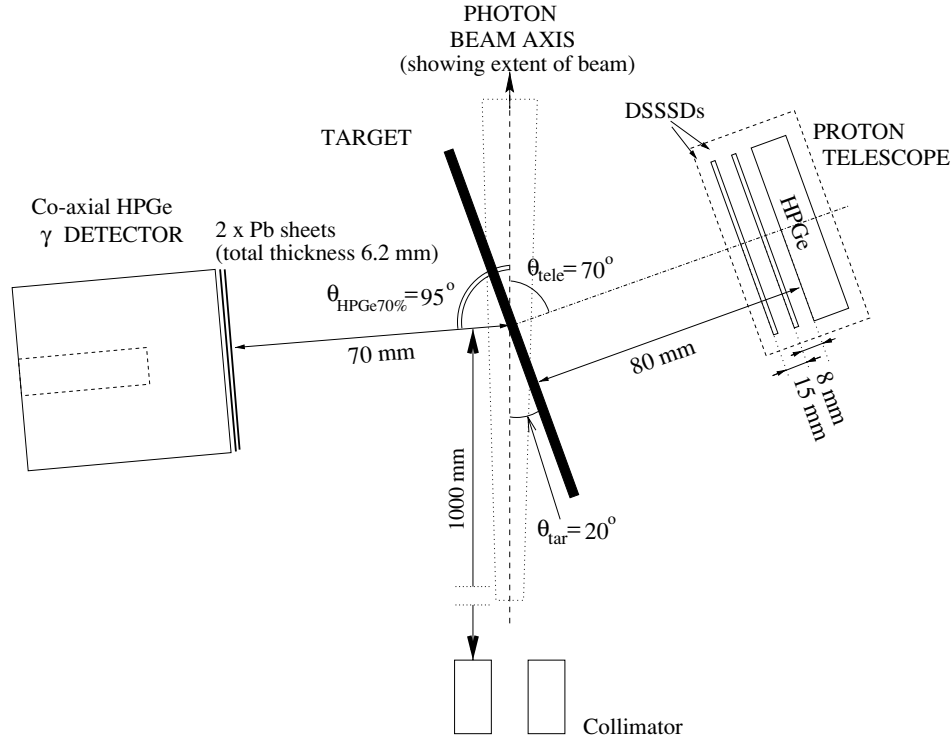


FIG. 1. Schematic diagram showing the plan view of the experimental setup.

II. EXPERIMENTAL METHOD AND ANALYSIS

The $^{12}\text{C}(\gamma, p\gamma')^{11}\text{B}$ experiment was carried out using the tagged photon facility of the MAX-lab [28]. The experimental setup is shown schematically in Fig. 1. The bremsstrahlung radiation γ beam was generated by a beam of $T_e = 92.3$ MeV electrons incident on $50\text{-}\mu\text{m}$ -thick Al radiators. The collimated γ beam had a diameter of ~ 32 mm at the target as measured using Polaroid film placed behind a Pb converter. The focal plane of the tagging spectrometer was instrumented with 64 plastic scintillators, which were used to tag photons in the range 49.5–70.2 MeV with an energy resolution of ~ 330 keV. Typical tagged photon rates were $\sim 3 \times 10^6$ photons s^{-1} . The tagging efficiency was measured several times throughout the experiment and remained roughly constant with an average value of 23.9%.

The target was a 100×100 mm rigid graphite slate (99.95% purity) of physical thickness ~ 2.5 mm (562.5 mg cm^{-2}) placed at $20.0^\circ \pm 0.5^\circ$ to the photon beam direction as shown in Fig. 1. An ~ 1 -mm (225 mg cm^{-2}) target was used for calibration of the proton telescope. Knocked-out protons were detected in a solid-state detector telescope (right-hand side of Fig. 1), which comprised two DSSSDs and a HpGe detector, which measured proton emission angles and energies, respectively. The DSSSDs were 50×50 mm and had 16 strips on each side. The HpGe had an active diameter of 49.5 mm and a thickness of ~ 9 mm. The Be entrance window had a thickness of ~ 500 μm . This detector telescope was placed at a mean angle of 70° to the beam direction (see Fig. 1) to minimize proton energy losses in the target.

The total experimental proton energy resolution, which was dominated by energy losses in the target, was estimated to be ~ 6 MeV. Used in combination with the very much higher resolution γ -ray data, this was adequate to determine the ^{11}B excitation energy regions associated with a particular γ ray. Because of the finite target spot, protons in the angular range $\theta_p = 35^\circ\text{--}105^\circ$ could be accepted and the telescope subtended a solid angle of ~ 300 msr. The full-width-half-maximum (FWHM) angular resolution varied from $\sim 8^\circ$ for central angles to $\sim 11^\circ$ at the extremes of the telescope acceptance.

Coincident γ rays from the decay of excited states in ^{11}B were observed using a coaxial HpGe detector (left-hand side of Fig. 1) that had a relative peak efficiency of 70% for the detection of 1.33 MeV γ -rays compared to a 7.62×7.62 cm Na(Tl) detector at 25 cm from a ^{60}Co source. This detector was placed with the front face 70 mm from the target at an angle of 95° to the beam direction (see Fig. 1) and subtended a solid angle of ~ 700 msr. The 95° angle was chosen because it corresponded to the mean angle at which ^{11}B nuclei in coincidence with protons detected in the DSSSDs-HpGe telescope were calculated to recoil. Although this choice resulted in the γ rays being significantly Doppler shifted in energy, it resulted in minimum Doppler broadenings of the peaks. Pb sheets of total thickness 6.2 mm were placed in front of the 70% HpGe to reduce the counting rate of low-energy γ rays. The gain of the γ -amplification chain was carefully monitored using a strong γ peak at 511 keV from the annihilation of positrons near the detector and pulses from a precision pulse generator set above the

γ -pulse range of interest. The gain was found to be stable within a few keV for the full period of the experiment, which lasted 21 days.

The signals from the proton HpGe detector, the DSSSDs and the HpGe γ detector were fed into CAMAC ADC modules. Timing signals for the HpGe detectors were obtained using constant fraction discriminators in conjunction with timing filter amplifiers. Timing information between the tagger and proton E detector and between the 70% HpGe γ detector and the proton E detector were recorded in TDCs. The FWHM time resolution obtained between the focal plane elements and the proton E detector was 1–2 ns. Although the FWHM time resolution obtained between the 70% HpGe γ detector and the proton E detector was only ~ 30 ns; this was adequate because the TDC spectrum contained a very low background from random coincidences.

The absolute efficiency of the 70% HpGe γ detector was determined using standard calibrated γ sources up to an energy $E_\gamma = 1.33$ MeV. The efficiency curve was extrapolated to $E_\gamma = 11$ MeV using the results of measurements made for a 32% relative efficiency Ge(Li) detector [29]. These results were considered to be sufficiently accurate for the present measurement, which was based primarily on the relative numbers of counts in neighboring peaks corresponding to the small γ -energy range $E_\gamma = 6.7$ – 7.3 MeV. Over this range, the absolute efficiencies differ by only small amounts and consequently it is reasonable to assume ratios of efficiencies have small errors. It should also be noted that the absolute cross sections presented in Sec. III were obtained by normalization to the absolute cross sections published in Refs. [22,25] and are not based on our HpGe γ -detector absolute efficiency estimates.

γ -ray line shapes were determined at 2.61 and 4.44 MeV using ^{228}Th and Am(Be) sources, respectively. Additional line shapes at 6.128 and 7.117 MeV were obtained by using the Am(Be) source inside a cylindrical Teflon holder [30,31]. Line shapes used to fit the $^{12}\text{C}(\gamma, p\gamma)^{11}\text{B}$ γ spectra were derived from these data by first decomposing each of the spectra into components corresponding to the photopeak, 1st escape peak, 2nd escape peak, a Compton continuum appropriate to the full energy of the γ ray, and Compton continua above the escape peaks arising from Compton scattering of the 511-keV annihilation quanta. The peaks were fitted using Gaussian functions, which were considerably wider than the intrinsic resolution of the detector for the 4.44 MeV line shape because of Doppler broadening. The Compton continua were calculated using a formula based on the Klein-Nishina theory [31,32]. An example of a decomposed line shape is shown in Fig. 2 and the fit to the 4.44 MeV γ -ray spectrum obtained using the Am(Be) source is shown in Fig. 3. Overall fits to these calibration spectra were good except in the regions close to the end points of the Compton continua, as can be seen in Fig. 2. This is thought to be because of multiple Compton scattering and considered not to be detrimental to the analysis presented in Sec. III because the spectra to be fitted mostly included events from γ rays with similar energies. The line shapes used in the fits were generated by summing all the components adjusted and weighted according to the observed trends in the calibration data and applying appropriate constraints such as

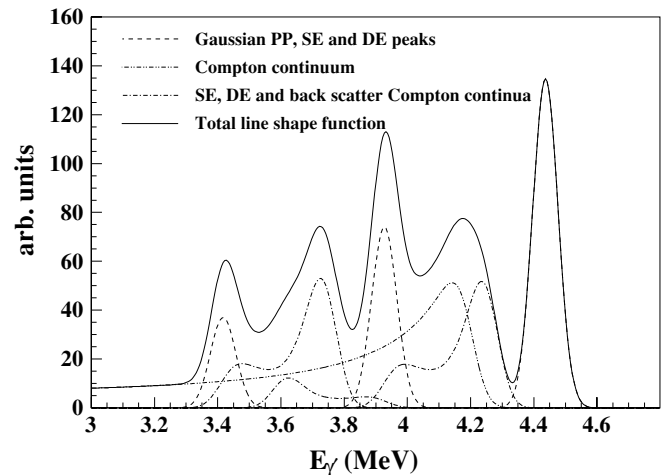


FIG. 2. Example of the γ -ray line shape used to fit the deexcitation γ -ray spectra.

keeping the ratio of areas under the 1st and 2nd escape peaks at the experimentally determined value.

III. ANALYSIS AND RESULTS

The data were analyzed to produce spectra showing ^{11}B excitation (E_{ex}) by analyzing each event according to the equation $E_{\text{ex}} = E_\gamma - T_p - T_r + Q_{gs}$, where E_γ is the energy of the tagged photon, T_p is the kinetic energy of the detected proton, T_r is the kinetic energy of the recoiling ^{11}B calculated using two-body kinematics, and Q_{gs} is the Q value for the reaction leading to the ^{11}B ground state. The higher histogram shown in the upper part of Fig. 4 was obtained by selecting events which gave counts within a narrow window centered around the sharp time peak in the proton-tagger TDC spectrum.

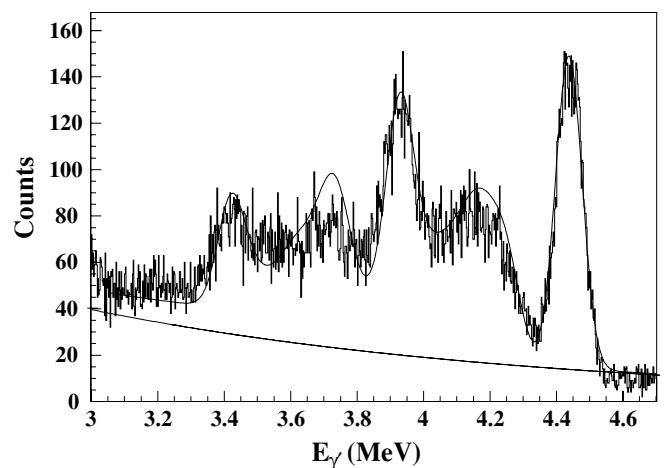


FIG. 3. Fit to the 4.439-MeV γ -ray spectrum obtained using an Am(Be) source inside a Teflon cylinder [30]. The poor resolution arises because the reaction $^9\text{Be}(\alpha, n)^{12}\text{C}^*$ results in Doppler broadening of the ^{12}C decay γ -ray spectrum. The exponential curve is used to simulate the background from detecting higher energy γ -rays, etc.

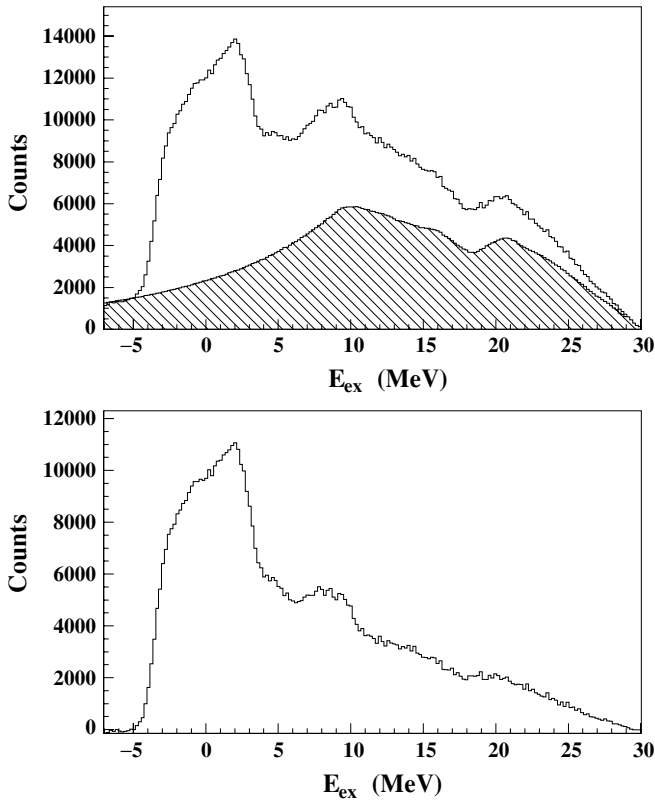


FIG. 4. Excitation energy spectrum for the $^{12}\text{C}(\gamma, p)^{11}\text{B}$ reaction obtained using a ~ 2.5 -mm-thick C target. The upper figure shows the true plus random coincidences spectrum together with a normalized random coincidences spectrum (hatched). The lower figure shows the result of subtracting the random coincidences spectrum. The resolution is $\Delta E_{\text{ex}} \sim 6$ MeV.

The hatched area (appropriately weighted) was obtained by considering events that gave rise to the flat portions of the proton-tagger TDC spectrum above and below the time peak. The lower part of Fig. 4 shows result of subtracting the hatched region from the higher histogram. The peaks at $E_{\text{ex}} \sim 0.0$ MeV and ~ 7.0 MeV correspond to strong excitation of the ground plus 2.12 MeV pair of states and the triplet of states at ~ 7 MeV consistent with a resolution of ~ 6 MeV. In the following, the events used to generate the higher histogram shown in upper part of Fig. 4 are referred to as the tagged data and correspond to incident photons in the energy range $E_{\gamma} = 49.5\text{--}70.3$ MeV. The events used to generate the hatched region of Fig. 4 are referred to as the random data. For the analysis based on all recorded events, which include those that give rise to the time peak and the flat background of the proton-tagger TDC random spectrum, we refer to the events as untagged data. In this case, the data correspond to incident photons in the approximate energy range $E_{\gamma} = 40\text{--}90$ MeV, which arises from the lower E_p detection threshold of the DSSSD/HpGe telescope and the bremsstrahlung end-point energy.

Doppler-shift-corrected spectra were determined for decay γ s observed in coincidence with protons for both the untagged and tagged data. For the untagged data, each event was analyzed as follows. The DSSSD/HpGe proton telescope information was used to determine the position on the target

where the tagged photon interacted, the kinetic energy of the proton and the direction of emission. Because the tagged photon energies were not available for individual events, a weighted mean $E_{\gamma} = 59.9$ MeV and a constant excitation energy of $E_{\text{ex}} = 6.8$ MeV was used for all events to calculate a ^{11}B recoil velocity and direction. A direction for the decay γ was obtained by assuming the interaction with the 70% HpGe detector occurred on the axis at a distance from the front face of 2.3 cm, which corresponds to the γ -attenuation length at $E_{\gamma} = 7$ MeV [33]. Using these data, the projection of the recoiling ^{11}B velocity along the decay- γ direction was determined and hence the fractional Doppler shift. The digital address corresponding to the decay γ was reduced by this fraction before being used to increment the spectrum. For decay γ s observed in the tagged data, a similar procedure was used except that the tagged photon energy, proton emission angle, and excitation energy information were used to calculate the ^{11}B recoil velocity and direction. No selection on regions of the excitation energy spectrum were applied because the base width of the peak because of the ~ 7 MeV triplet was very poorly defined. However, it should be noted that very few γ s were observed in coincidence with events that gave rise to $E_{\text{ex}} \sim 11$ MeV, which is approximately the upper limit expected for the broadened peak from the ~ 7 -MeV triplet. Examples showing the effects of applying the Doppler-shift corrections using tagged data are shown

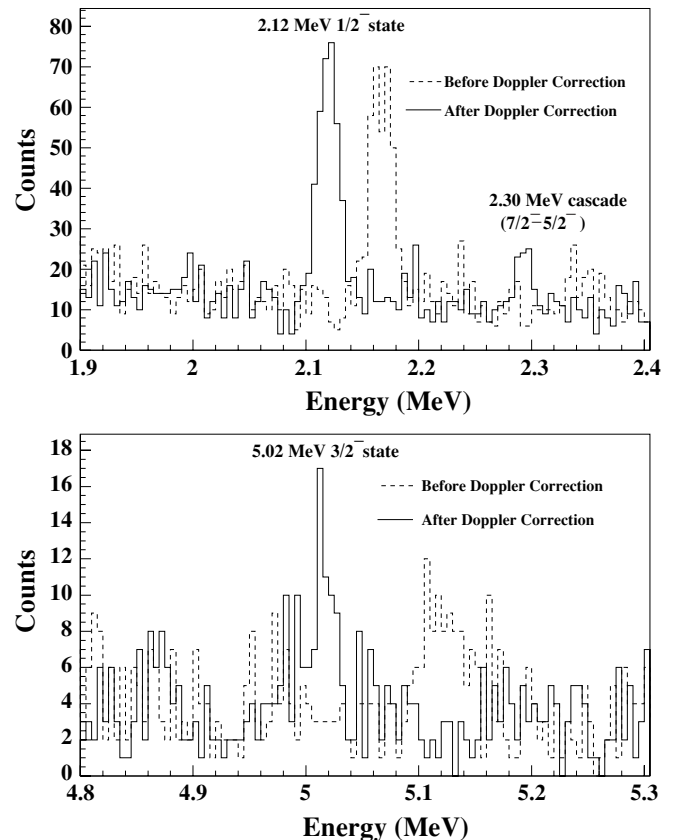


FIG. 5. Spectra showing the effect of applying the Doppler-shift correction procedure to the 2.12- and 5.02-MeV γ rays observed using the $^{12}\text{C}(\gamma, p\gamma)^{11}\text{B}$ tagged data. The data are presented in 5-keV bins.

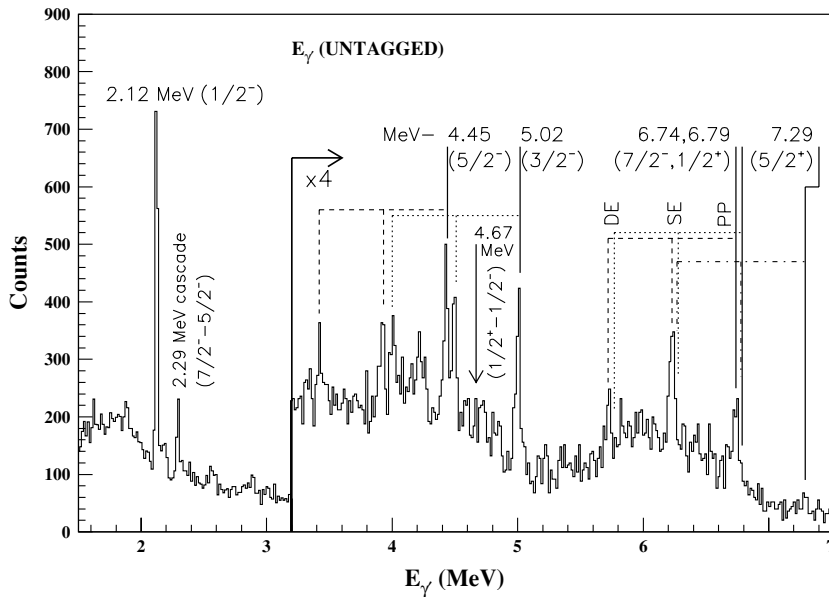


FIG. 6. Section of the Doppler-corrected γ spectrum obtained using the 70% HpGe detector in coincidence with protons to observe decay γ s from the $^{12}\text{C}(\gamma, p\gamma')^{11}\text{B}$ reaction. This spectrum was obtained using untagged data. The range of proton energies used in the analysis corresponded to a range of incident photon energies of approximately $E_\gamma = 40\text{--}90$ MeV.

in Fig. 5. Although these procedures only gave approximate Doppler-shift corrections for each event, they gave corrected spectra that on average corresponded approximately to a zero Doppler shift measurement and significantly reduced the Doppler broadening of the γ peaks. To have reduced the Doppler broadening further would have required a large position sensitive HpGe γ detector, which was not available at the time of the experiment. We note that such detectors are currently being developed and their use could significantly improve measurements of the type presented here.

The full energy spectra of decay γ s in coincidence with protons based on the untagged and tagged data using 15-keV-wide $E_{\gamma'}$ bins are shown in Figs. 6 and 7, respectively. Subtraction of random events on an event-by-event basis from the tagged spectrum shown in Fig. 7 gave rise to increased statistical uncertainties in the contents of each channel, which made it difficult to produce a meaningful fit to the data.

We therefore produced and analyzed a separate appropriately normalized γ' spectrum from the random events to determine the contribution to Fig. 7 from random events. The distribution of counts in the randoms spectrum, which was produced using the same procedure as for the spectrum shown in Fig. 7, is almost identical to that for Fig. 6, as would be expected because the untagged data contain $\sim 98\%$ random events. Selected regions of Fig. 6 are shown in Figs. 8 and 9, whereas Figs. 10 and 11 show the corresponding spectra from Fig. 7. These spectra show peaks corresponding to the decay γ s of interest as can be deduced from Table I. Peaks at 6.74, 6.79, and 7.29 MeV are from events where a member of the triplet decayed directly to the ground state. Peaks at 2.29 and 4.45 MeV from the cascade of the 6.74-MeV state through the 4.45-MeV state, which was used in the analysis of Kuzin *et al.* are clearly seen in Figs. 6 and 7. However, the 4.67-MeV decay γ from the cascade of the 6.79-MeV state through the

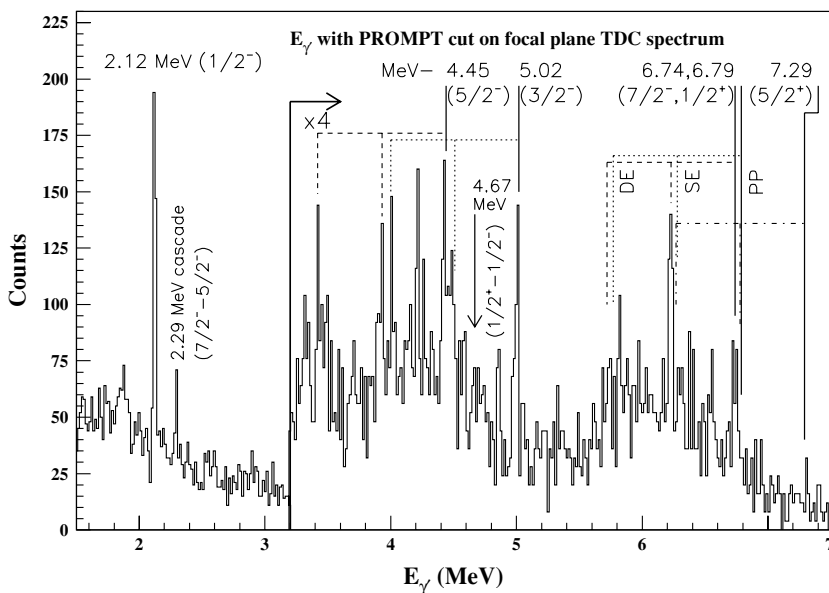


FIG. 7. Section of the Doppler-corrected γ spectrum obtained using the 70% HpGe detector in coincidence with protons to observe decay γ s from the $^{12}\text{C}(\gamma, p\gamma')^{11}\text{B}$ reaction. This spectrum was obtained using tagged data in coincidence with photons in the range $E_\gamma = 49.5\text{--}70.2$ MeV. This spectrum has not been corrected for random events included in the narrow proton-tagger time window.

TABLE I. Electromagnetic transitions in ^{11}B showing γ -branching ratios to the final states [27].

Initial state (MeV)	J^π	Branching ratios (%) to the final state						
		g.s.	2.12 MeV	4.45 MeV	5.02 MeV	6.74 MeV	6.79 MeV	7.29 MeV
2.12	$1/2^-$	100.0						
4.45	$5/2^-$	100.0						
5.02	$3/2^-$	85.6 ± 0.6	14.4 ± 0.6					
6.74	$7/2^-$	70.0 ± 2.0	≤ 3.0	30.0 ± 2.0	≤ 1.0			
6.79	$1/2^+$	67.5 ± 1.1	28.5 ± 1.1	≤ 0.04	4.0 ± 0.3			
7.29	$5/2^+$	87.0 ± 2.0	≤ 1	5.5 ± 1.0	7.5 ± 1.0			
7.98	$3/2^+$	46.2 ± 1.1	53.2 ± 1.2	≤ 0.06	≤ 0.09		≤ 0.1	≤ 1.0
8.56	$(3/2^-)$	56.0 ± 2.0	30.0 ± 2.0	5.0 ± 1.0	9.0 ± 1.0			
8.92	$5/2^-$	95.0 ± 1.0	≤ 1.0	4.5 ± 0.5	≤ 1.0	≤ 1.0	≤ 1.0	
9.19	$7/2^+$	0.9 ± 0.3		86.0 ± 2.3		12.5 ± 1.1	≤ 1.3	
9.27	$5/2^+$	18.4 ± 0.9		69.7 ± 1.4		11.9 ± 0.6	≤ 0.6	

2.12-MeV state, also used in the analysis of Kuzin *et al.* is not observed to any significant extent within the statistical accuracy of our measurement. The peaks at 2.12, 4.45, and 5.02 MeV are because of ground-state transitions from the levels at these energies, these being fed by a combination of transitions from the higher levels and direct feeding through the $^{12}\text{C}(\gamma, p)^{11}\text{B}$ reaction.

Figures 8–11 and the corresponding regions of the randoms spectrum were fitted using line shapes generated using the procedure described in Sec. II. An exponential background was used to account for tails on the γ -ray line shapes, incomplete containment of the γ energy deposited in the 70% HpGe detector from electron and bremsstrahlung losses, γ rays scattered into the detector from surrounding material, neutron detection, pile-up, random γ -proton coincidences, etc. These backgrounds were fixed using regions free of peaks above and below the fitted regions and interpolated into the fitted regions. An exponential shape was chosen to describe the backgrounds

because plots of all γ spectra (data and calibrations) made using a logarithmic scale for the counts per channel had the appearance of a straight line with peaks and Compton backgrounds superimposed on top. For the untagged spectra shown in Figs. 8 and 9, the positions of the γ line shapes, peak widths, and line-shape areas were allowed to vary within reasonable limits. To reduce the number of free parameters, the separation between the 6.74- and 6.79-MeV line shapes was fixed at 50 keV. The fits were obtained by searching for a minimum in χ^2 by considering all channels in the spectra as shown in Figs. 8–11. This procedure gave resolutions for peaks in the ~ 5 -MeV and ~ 7 -MeV regions of the spectra of 47.1 and 48.6 keV, respectively, which are consistent with our estimates of the residual Doppler broadenings. A similar procedure was used to fit the lower statistics tagged spectra shown in Figs. 10 and 11 except the line-shape positions and peak widths were fixed at the values obtained from the fits to the untagged data. This reduced the number of free parameters

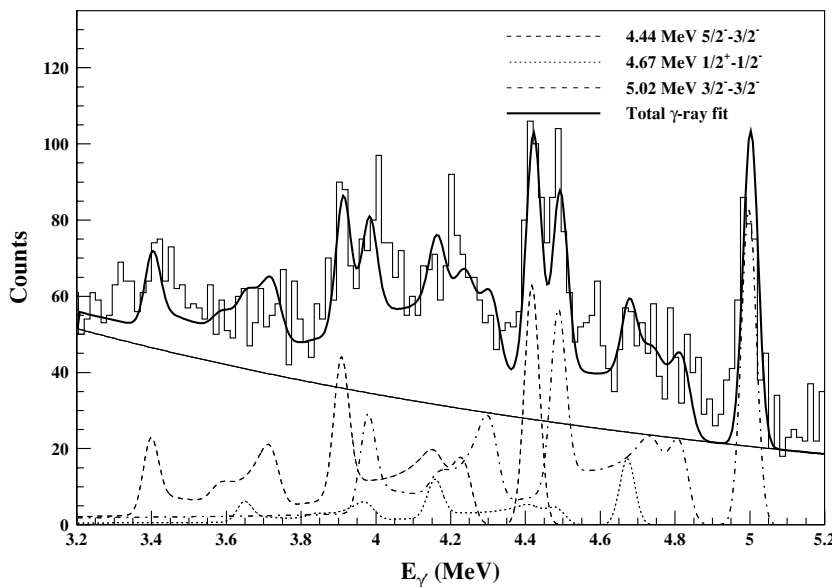


FIG. 8. Doppler-corrected γ spectrum for the $E_{\gamma'} \sim 5$ -MeV region obtained in coincidence with protons using untagged data from the $^{12}\text{C}(\gamma, p\gamma')^{11}\text{B}$ reaction. The range of proton energies used in the analysis corresponded to a range of incident photon energies of approximately $E_{\gamma} = 40$ – 90 MeV. The exponential curve is used to simulate the background from detecting γ -ray tails, etc.

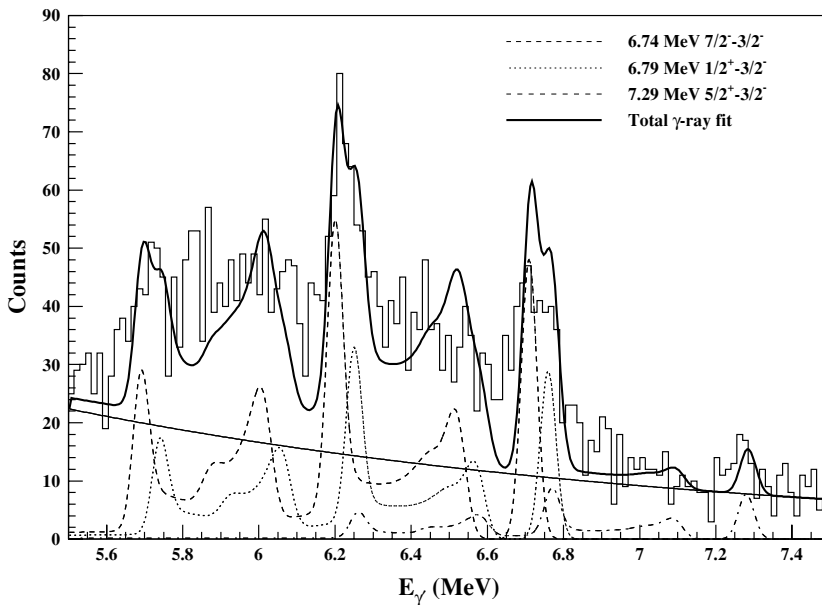


FIG. 9. Doppler-corrected γ spectrum for the $E_{\gamma'} \sim 7$ -MeV region obtained in coincidence with protons using untagged data from the $^{12}\text{C}(\gamma, p\gamma)^{11}\text{B}$ reaction. The range of proton energies used in the analysis corresponded to a range of incident photon energies of approximately $E_{\gamma} = 40$ – 90 MeV. The exponential curve is used to simulate the background from detecting γ -ray tails, etc.

used in the fitting procedure and can be justified because the tagged data are a subset of the untagged data. However, because the initial fits based on considering all channels in Figs. 10 and 11 gave shallow χ^2 minima and unconvincing fits, the intensities of the individual γ s were modified starting with the initial values to give the best fits to all channels within ± 75 keV of the main peaks.

The dashed, dotted, and dash-dot lines shown in Figs. 8 and 11 show the line shapes for the individual γ s and the solid lines are the sums of the exponential curve and individual γ line shapes. The poor fits to some regions of the Compton continua may be because of the effects of multiple Compton scattering considered in Sec. II. The areas under the individual line shapes, corrected by small amounts to account for the variations in γ -detection efficiency, were used to determine the relative intensities of the γ s in the spectra.

The analysis described as follows depends on the levels of interest being populated directly by the $^{12}\text{C}(\gamma, p)^{11}\text{B}$ reaction and not fed by γ s from more highly excited states. In considering this we noted that the untagged spectrum (Fig. 6), which includes events from a wider range of ^{11}B excitation energies, looks similar to the tagged spectrum (Fig. 7). We also produced the spectrum shown in Fig. 12 using tagged events from the range $E_{\gamma} = 60.7$ – 70.2 MeV and gated around the broad 7-MeV triplet peak in the missing energy spectrum. Tagged photons from the higher energy half of the focal plane detector array were chosen to ensure that protons leading to states above ~ 10 MeV, for which the γ -decay strengths are expected to be small but not well established, were well above the threshold energy for detecting protons. From a comparison of Figs. 12 and 11 it is evident that, within the statistical accuracy of the measurement, the

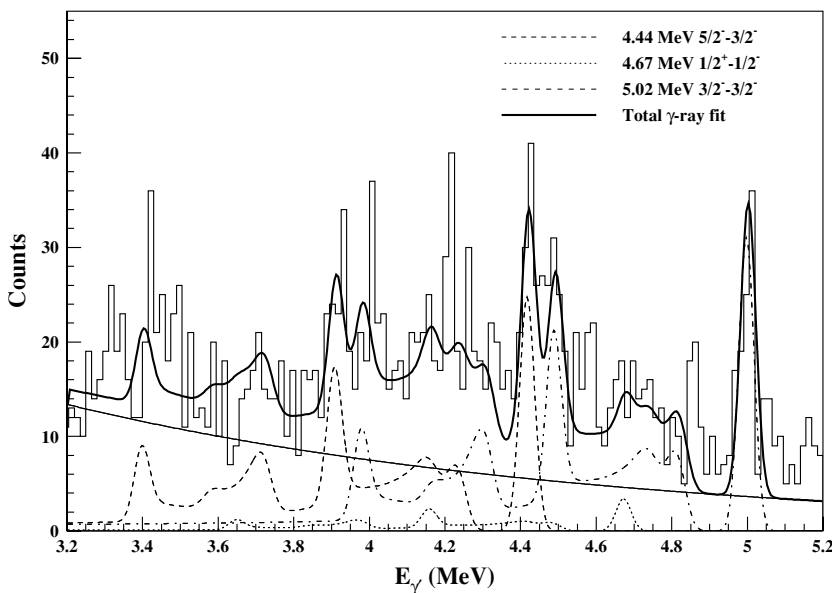


FIG. 10. Doppler-corrected γ spectrum for the $E_{\gamma'} \sim 5$ -MeV region obtained in coincidence with protons using tagged data from the $^{12}\text{C}(\gamma, p\gamma)^{11}\text{B}$ reaction. The tagged photons covered the range $E_{\gamma} = 49.5$ – 70.2 MeV. The exponential curve is used to simulate the background from detecting γ -ray tails, etc. This spectrum has not been corrected for random events included in the narrow proton-tagger time window.

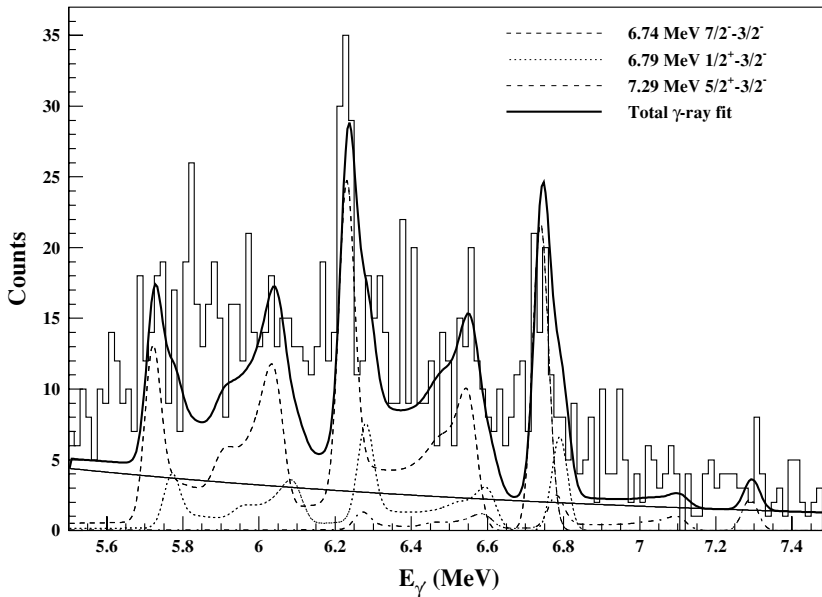


FIG. 11. Doppler-corrected γ spectrum for the $E_{\gamma'} \sim 7$ -MeV region obtained in coincidence with protons using tagged data from the $^{12}\text{C}(\gamma, p\gamma')^{11}\text{B}$ reaction. The tagged photons covered the range $E_{\gamma} = 49.5\text{--}70.2$ MeV. The exponential curve is used to simulate the background from detecting γ -ray tails, etc. This spectrum has not been corrected for random events included in the narrow proton-tagger time window.

ratios of the peak areas for the 6.74 to 7.29 MeV γ s are similar. Based on these results, it was concluded that significant feeding of the triplet of states by γ decays from higher lying states is unlikely. This conclusion is strengthened by other considerations as follows. The 6.74-MeV state is the only member of the ~ 7 -MeV triplet that could be significantly fed by known γ decays from higher states. The higher states involved are at 9.19 and 9.27 MeV, which if populated would decay to the 6.74-MeV state by γ s at $E_{\gamma'} = 2.45$ and 2.53 MeV, respectively [27]. However, these states also decay to the 4.45-MeV level with higher branching ratios, which would give γ s at $E_{\gamma'} = 4.75$ and 4.83 MeV, respectively. Spectra 6 and 7 show no evidence for γ peaks at any of these four energies. Also, previous high-resolution $^{12}\text{C}(\gamma, p)^{11}\text{B}$ data [26,34] show that levels at $E_{\text{ex}} \sim 9$ MeV are populated very weakly. It was concluded, therefore, that although the

missing energy resolution was only ~ 6 MeV, reliable relative populations of the triplet states could be obtained through an analysis of the tagged data shown in Figs. 10 and 11, under the assumption that the populations are in proportion to the observed γ intensities.

The intensities of the individual γ s shown in Figs. 10 and 11 were reduced to account for the contribution of random coincidences to the spectrum using results from the fits to the randoms spectrum. The average reduction in counts was 42%. The randoms corrected intensities divided by the detection efficiency and the branching ratio (see Table I) are presented as R_i^U in Table II. In keeping with the analysis of Kuzin *et al.*, the results are normalized to the yield of the 6.74-MeV state. The error in each R_i^U includes a statistical component obtained from the fitting procedures, combined in quadrature with the error in the branching ratio as shown in Table I. Our results are based on the strong ground-state transitions with the exception of the result shown as 6.79* MeV, which is based on the transition to the 2.12-MeV ($1/2^+$) state. The result for the 5.02-MeV state was reduced by a calculated small amount to account for feeding from the 6.79- and 7.29-MeV states shown in Table I.

Table II also shows in column 5 the data of Kuzin *et al.* [20], which were obtained using a tagged photon range of $E_{\gamma} = 50\text{--}70$ MeV. From a comparison of our results with these data, it is evident that both measurements show the 6.74-MeV state to be the most strongly excited member of the ~ 7 -MeV triplet. However, our R_i^U result for the 7.29-MeV state does not agree with the result taken from Kuzin *et al.* A most likely explanation is that the differences arise from γ -proton angular correlations. To consider this possibility, we investigated the effects that γ -proton angular correlations could have on our measurement and that of Kuzin *et al.* The chosen axis of quantization was the recoiling ^{11}B nucleus direction, which for our measurement was on average parallel to the central axis of the 70% HpGe detector. For the measurement of Kuzin *et al.* the axis of symmetry of the cone of recoiling ^{11}B nuclei was at an angle of 90° to the γ detectors. Because calculations on the

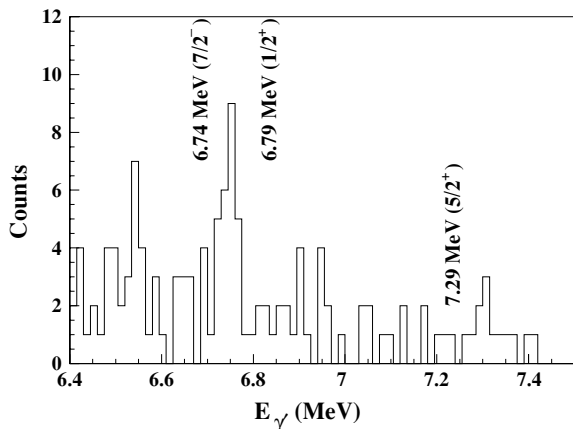


FIG. 12. Doppler-corrected γ spectrum for the $E_{\gamma'} \sim 7$ -MeV region obtained in coincidence with protons from the $^{12}\text{C}(\gamma, p\gamma')^{11}\text{B}$ reaction corresponding to the excitation energy range $E_{\text{ex}} = 3.3\text{--}10.6$ MeV. The tagged photons covered the range $E_{\gamma} = 60.7\text{--}70.2$ MeV. This spectrum has not been corrected for random events included in the narrow proton-tagger time window.

TABLE II. Relative populations of levels in ^{11}B following the $^{12}\text{C}(\gamma, p)^{11}\text{B}$ reaction, including the effects of angular correlations. The R_i^C populations shown in columns 5 and 7, which are corrected for angular correlation effects, are renormalized relative to the population of the 6.74 MeV state. The results labelled 6.79* were derived from the transition to the 2.12 MeV $J^\pi = 1/2^-$ state.

Level MeV	J^π	$P_i/P_{6.74} = R_i^U$ (uncorrected)	$W(\theta_{\gamma'} = 0^\circ)$	$P_i/P_{6.74} = R_i^C$ (corrected)	R_i^U Kuzin <i>et al.</i> (uncorrected)	$W(\theta_{\gamma'} = 90^\circ)$	R_i^C Kuzin <i>et al.</i> (corrected)
5.02	$3/2^-$	0.73 ± 0.22	1.279 ± 0.078	1.01 ± 0.29	0.92 ± 0.10	0.880 ± 0.039	0.75 ± 0.09
6.74	$7/2^-$	1.00	1.797 ± 0.206	1.00	1.00	0.717 ± 0.053	1.00
6.79	$1/2^+$	0.15 ± 0.13	1.00	0.27 ± 0.23		1.00	
6.79*	$1/2^+$	0.08 ± 0.11	1.00	0.14 ± 0.19	0.23 ± 0.03	1.00	0.16 ± 0.03
7.29	$5/2^+$	0.06 ± 0.06	0.750 ± 0.097	0.14 ± 0.14	0.35 ± 0.05	1.136 ± 0.048	0.22 ± 0.04

$^{12}\text{C}(\gamma, p)^{11}\text{B}$ showing ^{11}B spin alignments were not available, we made estimates of the γ -proton angular correlation effects as follows. Assuming the reaction proceeds by a direct reaction mechanism, the angular momentum transferred to the residual nucleus is, from semiclassical arguments, $\mathbf{L} = \mathbf{r} \times \mathbf{p}$, where \mathbf{r} is the interaction point relative to the center of the target nucleus and \mathbf{p} is the transferred (recoil) momentum. It follows therefore that the projection of \mathbf{L} onto the recoil direction \mathbf{p} is $M \sim 0$ [35]. Because the incident tagged photon, which is spin aligned with the $M = \pm 1$ projections along its direction of motion, moves in a direction that is approximately perpendicular to the recoil direction, the projection of the spin on the recoil direction will also lead to an L-magnetic substate population of $M \sim 0$. However, the proton carries a spin of $S = 1/2$ and moves in the opposite direction to the recoiling nucleus. Hence, assuming the reaction does not lead to significant proton spin polarization, it is reasonable to expect from spin conservation arguments that the spin J of the recoiling ^{11}B nuclei will be mainly aligned in the $M = \pm 1/2$ substates relative to the recoil direction. Based on this assumption, we calculated the expected angular correlation [36] functions $W(\theta_{\gamma'}) = \sum_k a_k Q_k P_k(\cos \theta_{\gamma'})$ relative to the recoil direction, where k are even, $P_k[\cos(\theta_{\gamma'})]$ are Legendre polynomials, and the Q_k account for the finite size of the detector. The a_k coefficients were calculated using tables presented in Ref. [36] and information on the multipolarities taken from Ref. [27]. Reasonable values for the Q_k for both our measurement and that of Kuzin *et al.* were taken as $Q_2 = 0.80$, $Q_4 = 0.40$, and $Q_6 = 0.05$, based on the work of Refs. [37,38]. Errors arising from the experimental errors in the multipole mixing ratios [27] and an estimated $\pm 10\%$ error in the dominant angular correlation attenuation coefficient Q_2 were included in these calculations. Values of $W(\theta_{\gamma'} = 0^\circ)$ and $W(\theta_{\gamma'} = 90^\circ)$ were calculated and divided into the R_i^U results of this measurement and those of Kuzin *et al.* respectively, to give the R_i^C data as shown in Table II. It is interesting to note that the normalized results for the 7.29-MeV state are in much closer agreement following application of the angular correlation factors.

Absolute cross sections at $\theta_p = 70^\circ$ were obtained in exactly the same way as described by Kuzin *et al.* by normalization to the data of Refs. [22,25], which give an average value of $7.52 \mu\text{b sr}^{-1}$ for the $^{12}\text{C}(\gamma, p)^{11}\text{B} \sim 7\text{-MeV}$ triplet cross section over the range $E_\gamma = 50\text{--}70$ MeV. Hence the two data sets, which are presented in Table III, can be directly compared. It should be noted though that the errors do not include system-

atic errors of approximately $\pm 20\%$ associated with the measurements of Refs. [22,25]. Based on either the uncorrected or corrected data, it can be concluded that both our experiment and that of Kuzin *et al.* show the 6.74 ($7/2^-$) to be the most strongly excited member of the $\sim 7\text{-MeV}$ triplet. Good agreement is also observed between the corrected cross sections for populating the 7.29-MeV ($5/2^+$) and 6.79 ($1/2^+$) states.

The results presented in Table II suggest that the inclusion of γ -proton angular correlation effects is a necessary step in the analysis. Clearly, it would be desirable to have measurements of these effects or better estimates of the alignments expected for the residual nuclei than the semiclassical method described here. Regarding the $M = \pm 1/2$ assumptions made in our analysis, we point out that in an unpublished trial measurement of the $^{16}\text{O}(\gamma, p\gamma')^{15}\text{N}$ reaction immediately following the $^{12}\text{C}(\gamma, p\gamma')^{11}\text{B}$ study, the known strongly populated 6.32 MeV ($3/2^-$) state [39] gave rise to relatively few counts in the spectrum observed using the 70% HpGe detector. However, Kuzin *et al.* observed a strong 6.32-MeV peak in the γ' spectrum using their geometry [40]. These results are consistent with the assumption that the J of the ^{15}N nuclei were aligned in the $M = \pm 1/2$ substates relative to the recoil direction, which would give $W(\theta_{\gamma'} = 0^\circ) = 0$ and $W(\theta_{\gamma'} = 90^\circ) = 1.5$ for the $3/2^- \rightarrow 1/2^+$ ground-state $E1$ transition relative to the ^{15}N recoil direction. It was these results that alerted us to the possibility of strong angular correlation effects. In view of this, we assume the corrected results of Table III to be more appropriate than the uncorrected results for comparison with theoretical models.

TABLE III. Normalized cross sections at $\theta_p = 70^\circ$ for exciting resolved members of the triplet of states in ^{11}B at ~ 7 MeV determined using the $^{12}\text{C}(\gamma, p\gamma')^{11}\text{B}$ reaction. The data shown in the columns marked Uncorrected and Corrected were derived using the R_i^U and R_i^C results of Table II, respectively. Our results for the 6.79-MeV state are based on the averages of the results labeled 6.79 and 6.79* in Table II.

Level MeV	J^π	$d\sigma/d\Omega$ Uncorrected $\mu\text{b sr}^{-1}$	$d\sigma/d\Omega$ Corrected $\mu\text{b sr}^{-1}$	$d\sigma/d\Omega$ (Kuz.) Uncorrected $\mu\text{b sr}^{-1}$	$d\sigma/d\Omega$ (Kuz.) Corrected $\mu\text{b sr}^{-1}$
6.74	$7/2^-$	6.37 ± 0.70	5.61 ± 1.18	4.76 ± 0.82	5.41 ± 0.93
6.79	$1/2^+$	0.76 ± 0.51	1.12 ± 0.75	1.08 ± 0.19	0.92 ± 0.23
7.29	$5/2^+$	0.38 ± 0.38	0.78 ± 0.78	1.66 ± 0.29	1.19 ± 0.32

Kuzin *et al.* compared their results to a revised calculation by Ryckebusch, which is based on a model described in an earlier article [19]. In this model, it is assumed that ground-state correlations are present in ^{12}C and excitation via the two-body part of the nuclear current operator takes place through photon absorption on meson exchange currents. This gives a natural explanation for the strong excitation of $2p$ - $1h$ states by photonuclear reactions. The revised calculation included the addition of Δ currents to the two-body part of the nuclear current operator, although this was found to be relatively unimportant at the photon energies used. Also, $1h$ excitations were included, which were assumed to arise from a small occupation of the $1f_{7/2}(7/2^-)$, $1d_{5/2}(5/2^+)$, and $2s_{1/2}(1/2^+)$ single-particle orbits in the ^{12}C ground state. Spectroscopic factors of $S=0.017$, 0.010 , and 0.0038 , associated respectively with each of these components, were taken from $^{12}\text{C}(e, e'p)^{11}\text{B}$ measurements [41]. In spite of the small spectroscopic factors, the calculations indicated that the inclusion of $1h$ excitation is important because the two-body terms were found to strongly interfere both constructively and destructively with the one-body term. The results of this calculation are shown in Fig. 13 where they are compared to the corrected results of Table III. The points at $\theta_p \sim 120^\circ$ are taken directly from Kuzin *et al.* and have not been corrected for angular correlation effects because it is not clear how to estimate the ^{11}B spin alignment in this case.

From Fig. 13, it is evident that the angular-correlation corrected new results and those of Kuzin *et al.* are all in reasonable agreement with the $^{12}\text{C}(\gamma, p)^{11}\text{B}$ calculations at $\theta_p \sim 70^\circ$. All experimental results and the calculation show the 6.74-MeV $7/2^-$ state of the $E_{\text{ex}} \sim 7$ -MeV triplet as having the highest cross section. Also both sets of experimental results for the 7.29-MeV $5/2^+$ and 6.79-MeV $1/2^+$ states indicate that the cross sections are $\sim 1 \mu\text{b sr}^{-1}$, which agree with the calculated

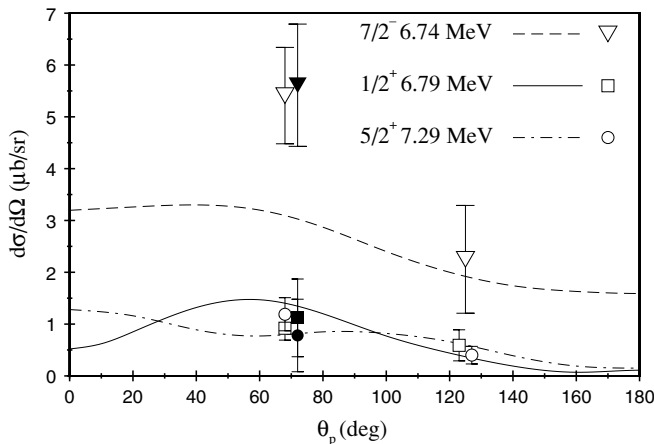


FIG. 13. Average differential cross sections for members of the ~ 7 -MeV triplet of states populated by the $^{12}\text{C}(\gamma, p)^{11}\text{B}$ reaction over the energy range $E_\gamma = 50$ – 70 MeV compared to theoretical results calculated by Ryckebusch for an average $E_\gamma = 60$ MeV and presented in Kuzin *et al.* [20]. Filled and open symbols are results from this experiment and that of Kuzin *et al.*, respectively. The theory curves are based on the model of Ryckebusch *et al.* [19], and include one- and two-body nuclear currents, pion exchange, and Δ currents.

results. In view of these considerations, we conclude that our new measurement provides valuable complementary data to that of Kuzin *et al.* and gives further support to the model of Ryckebusch, which includes nuclear terms from both one- and two-body currents and assumes the photon is absorbed on meson exchange currents [19].

A final point to note is that the sum of the theory curves for populating all members of the triplet of states at $\theta_p \sim 70^\circ$ gives a smaller value than the sum of the experimental cross sections. Although scaling of the calculations by a common factor cannot be justified because of the interference effects, it is evident that multiplying the theory curves by a factor of approximately 1.5 would give good overall agreement with our data and most points of Kuzin *et al.* This suggests that it would be worthwhile to revisit this problem theoretically and investigate if a better overall theoretical fit can be achieved.

IV. CONCLUSIONS

The $^{12}\text{C}(\gamma, p\gamma')^{11}\text{B}$ measurement reported here shows that residual nucleus states separated in energy by ~ 50 keV can be resolved by observing decay γ rays using a HpGe γ detector in close proximity to the target. However, the resolution that can be obtained is very much limited by Doppler broadening effects, which for our measurement was minimized by using an experimental setup in which the central axis of the HpGe detector was along the mean ^{11}B recoil direction. A more versatile setup would require position-sensitive HpGe γ detectors, which are currently available. Using such detectors, it should be possible to resolve states separated by a few keV. A disadvantage of both the geometry used here and that of Kuzin *et al.* is that the results can be biased by γ -proton angular correlations. Arguments presented here suggest that residual nuclei recoiling at $\theta \sim 90^\circ$ following a (γ, p) reaction on a $J^\pi = 0^+$ target nucleus will give rise to the J of the residual nuclei being approximately aligned relative to the recoil direction in the $M = \pm 1/2$ substates. Corrections were made to both the results presented here and those of Kuzin *et al.* based on this assumption. Clearly this assumption should be checked in future, both experimentally and using theoretical models, especially as it is anticipated that the observation of decay γ s to resolve the final states of photonuclear reactions will become more widely used.

The results presented here provide valuable complementary data to the measurement of Kuzin *et al.* and confirm the main conclusion that the 6.74-MeV $7/2^-$ state is the most strongly excited member of the ~ 7 -MeV triplet observed using the $^{12}\text{C}(\gamma, p)^{11}\text{B}$ reaction at photon energies above the giant dipole resonance region. A comparison of the combined data to the calculations of Ryckebusch presented by Kuzin *et al.* gives further support to the model [19], which assumes that the reaction takes place on both one- and two-body nuclear currents and the photons are predominantly absorbed on meson exchange currents. It is pointed out that a simple scaling up of the calculations would bring the results into closer agreement with the new experimental data. In view of this, it is suggested that it may be worthwhile to revisit the theoretical model to investigate if a better overall fit to the data can be achieved.

ACKNOWLEDGMENTS

The authors acknowledge the outstanding support of the MAX-lab staff. The support of the U.K. Engineering and Physical Sciences Research Council through the provision of

research grants and the Ph.D. studentship of S. A. Morrow is gratefully acknowledged. The Lund group acknowledge the financial support of the Swedish Research Council, the Knut and Alice Wallenberg Foundation, the Crafoord Foundation, and the Royal Physiographic Society in Lund.

-
- [1] A. E. L. Dieperink and P. K. A. de Witt Huberts, *Annu. Rev. Nucl. Part. Sci.* **40**, 239 (1990).
- [2] P. K. A. de Witt Huberts, *J. Phys. G* **16**, 507 (1990).
- [3] G. van der Steenhoven, *Nucl. Phys.* **A527**, 17c (1991).
- [4] L. Lapikas, *Nucl. Phys.* **A553**, 297c (1993).
- [5] J. J. Kelly, *Adv. Nucl. Phys.* **23**, 75 (1996).
- [6] D. Branford *et al.*, *Phys. Rev. C* **63**, 014310 (2000), and references therein.
- [7] E. C. Aschenauer *et al.*, *Phys. Lett.* **B389**, 470 (1996).
- [8] D. G. Ireland and G. van der Steenhoven, *Phys. Rev. C* **49**, 2182 (1994).
- [9] L. J. de Bever *et al.*, *Phys. Rev. C* **58**, 981 (1998).
- [10] J. S. Levinger, *Phys. Rev.* **84**, 43 (1951); *Phys. Lett.* **B82**, 181 (1979).
- [11] L. Van Hoorebeke *et al.*, *Phys. Rev. C* **42**, R1179 (1990).
- [12] D. A. Sims *et al.*, *Phys. Rev. C* **45**, 479 (1992); L. Van Hoorebeke, D. Ryckbosch, R. vandeVyver, F. Desmet, J. O. Adler, B. E. Andersso, L. Isaksson, A. Sandell, B. Schroder, and K. Ziakas, *ibid.* **45**, 482 (1992).
- [13] G. van der Steenhoven and H. P. Blok, *Phys. Rev. C* **42**, 2597 (1990).
- [14] J.P. McDermott, E. Rost, J. R. Shepard, and C. Y. Cheung, *Phys. Rev. Lett.* **61**, 814 (1988).
- [15] G. M. Lotz and H. S. Sherif, *Nucl. Phys.* **A537**, 285 (1992).
- [16] J. I. Johansson, H. S. Sherif, and G. M. Lotz, *Nucl. Phys.* **A605**, 517 (1996).
- [17] J. I. Johansson and H. S. Sherif, *Phys. Rev. C* **56**, 328 (1997).
- [18] A. Meucci, C. Giusti, and F. D. Pacati, *Phys. Rev. C* **64**, 064615 (2001).
- [19] J. Ryckebusch, K. Heyde, L. Machenil, D. Ryckbosch, M. Vanderhaeghen, and M. Waroquier, *Phys. Rev. C* **46**, R829 (1992).
- [20] A. Kuzin *et al.*, *Phys. Rev. C* **58**, 2167 (1998).
- [21] A. C. Shotter *et al.*, *Phys. Rev. C* **37**, R1354 (1988).
- [22] S. V. Springham *et al.*, *Nucl. Phys.* **A517**, 93 (1990).
- [23] D. G. Ireland *et al.*, *Nucl. Phys.* **A554**, 173 (1993).
- [24] A. W. Rauf, Ph.D. thesis, University of Edinburgh, 1996 (unpublished).
- [25] H. Ruijter, J. O. Adler, B. E. Andersson, K. Hansen, L. Isaksson, B. Schroder, J. Ryckebusch, D. Ryckbosch, L. Van Hoorebeke, and R. E. Van de Vyver, *Phys. Rev. C* **54**, 3076 (1996).
- [26] E. C. Aschenauer *et al.*, *Nucl. Phys.* **A615**, 33 (1997).
- [27] F. Ajzenberg-Selove, *Nucl. Phys.* **A506**, 1 (1990).
- [28] J-O. Adler *et al.*, *Nucl. Instrum. Methods* **A294**, 15 (1990).
- [29] W. J. Vermeer *et al.*, *Phys. Lett.* **B217**, 28 (1989).
- [30] K. J. King and T. L. Johnson, *Nucl. Instrum. Methods* **227**, 257 (1984).
- [31] G. F. Knoll, *Radiation Detection and Measurement*, 2nd ed. (J. Wiley and Sons, 1989).
- [32] S. M. Shafroth *Scintillation Spectroscopy of Gamma Radiation* (Gordon and Breach, 1967), Vol. 1.
- [33] Yung-Su Tsai, *Rev. Mod. Phys.* **46**, 815 (1974).
- [34] I. Bobeldijk, Ph.D. thesis, University of Utrecht (1992).
- [35] F. A. B. Clegg and G. R. Satchler, *Nucl. Phys.* **27**, 431 (1961).
- [36] H. J. Rose and D. M. Brink, *Rev. Mod. Phys.* **39**, 306 (1967).
- [37] W. G. Winn and D. G. Sarantities, *Nucl. Instrum. Methods* **66**, 61 (1968).
- [38] K. Siegbahn *α -, β - and γ -ray Spectroscopy*, Vol. 2 (North-Holland, Amsterdam, 1965).
- [39] G. J. Miller *et al.*, *Nucl. Phys.* **A586**, 125 (1995).
- [40] A. Kuzin *et al.*, MAX-lab activity report, Lund University, Sweden (1996) (unpublished).
- [41] G. van der Steenhoven *et al.*, *Nucl. Phys.* **A484**, 445 (1988).